The Nature of Seat-ligand Fitting in Coordination Space. Part 1. An Introduction of 'Coordination Seat'

LI XING-FU*, SHEN TIAN-GI, GUO AO-LING, SHUN GUANG-LI and SUN PENG-NIAN

Application Department, The Institute of High Energy Physics, Academia Sinica, Beijing P.O. Box 2732, China

(Received June 9, 1986; revised November 13, 1986)

Abstract

The concept of 'Seat' is introduced to study steric packing quantitatively. Coordination space is analysed into a series of cone seats. Degeneracy, splitting, transformation and inversion of interlocking seats were studied with the seat level diagrams.

Steric isomerism is described with different seat level diagrams. In weak covalent compounds, the isomer, with the maximum *SAS* of the occupied seats, is more favourable for ligand packing. The difference between the largest vacant seat and the smallest occupied seat is also suggested as a criterion for estimating stable isomers.

Introduction

Although steric packing in coordination and organometallic chemistry has been recognized as an important factor, it has nevertheless been neglected in quantitative studies. The major problem is that steric packing is not the unique factor influencing molecular structures. Other factors, such as bonding, often prevail so that it is quite difficult to observe ideal steric packing except in some ionic lattices.

Nevertheless there have been continued efforts towards this objective. Tolman made the first attempt to quantify steric effects [1, 2]. More recently the concept of solid angle has been used to describe steric packing [3–7]. The Packing Saturation Rule (the so-called *SAS* rule) [8–10] and the Packing Centre Rule [9] have been reported. Molecular geometry [11, 12] and some reaction processes [13] have been explained quantitatively in terms of steric arrangement. However the treatments are still empirical. A more general and fundamental understanding is required. In the present paper, we introduce the geometrical analysis of coordination space and discuss briefly its application in structural chemistry.

*Author to whom correspondence should be addressed.

The currently adopted concept 'coordination site' refers only to a location of metal–ligand bonding in the coordination sphere. It does not indicate the steric hindrance, or geometrical restrictions, of the location. We thus introduce 'coordination seat' to describe the site quantitatively. In the unit sphere treatment [9], 'site' refers to a point whereas 'seat' refers to an area.

1. Seat Analysis

The coordination space around the central metal ion can be analysed into an infinite number of cone seats with the metal ion at their joined apex. In analysis at a certain symmetry, n_1 of the largest seats (*i.e.* the first order ones) which interlock with each other are derived first and n_2 of the next largest seats are derived from the holes among the first ones. The analysis continues to the third and the higher order ones. If we use the symbol S_i to represent the fan angle of the ith order seats, then we have

$$4\pi = 2\pi \sum_{i=1}^{\infty} n_i(1 - \cos S_i) \quad (1)$$

where 4π represents the solid angle of the whole space.

The process of seat analysis is illustrated using tetrahedral symmetry as an example (Fig. 1). The first order seats with $S_1 = 54.74°$ are located at the four apices of the tetrahedron whereas the second order seats with $S_2 = 15.5°$ are located at the centre of each triangular face of the tetrahedron. The third order seats are located in the holes among every two of the first order seats and one of the second order seats. Although such an analysis could be carried out infinitely, the seats which are smaller than a real ligand are less important. (A hydrogen atom, with its Van der Waal's radius of 1.2 Å and its distance 3 Å from the central atom, needs a seat larger than 23.6° ($S_H = \sin^{-1}(1.2/3)$).)

For convenience, we have introduced the 'Seat Level Diagram' (Fig. 2 and Table I) to describe the

0020-1693/87/$3.50

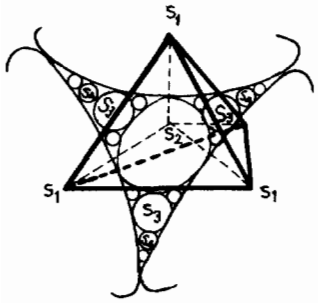

Fig. 1. Seat analysis for a tetrahedron.

seat analysis. Each seat is represented by a short line, which is arranged upwards in the sequence of size. The large seats are below the small ones, the infinite small seat (zero seat) is represented by a dotted line at the top. The symmetry of the first order seats is placed below the seat levels. The fan angle of the seat, expressed in S_i, is on the right-hand side of the level and its position has been put on the left-hand side. The ligands accommodated in the seats are written in above the corresponding seats. When the seat is empty it is written as an H.

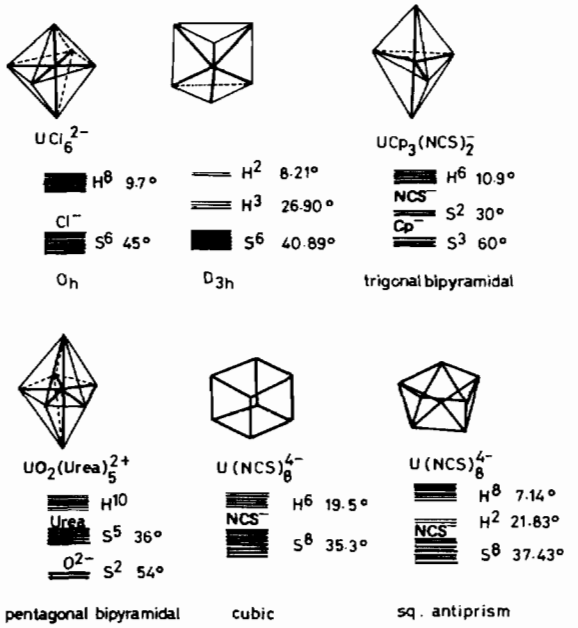

Fig. 2. Seat analysis and the corresponding seat level diagrams of the most common structural patterns.

2. Degeneracy and Splitting of the Seat Levels

In certain symmetries, the seat levels of identical seats are degenerate. For example, in T_d symmetry both the seat levels of the four first order seats and those of the four second order seats possess four-fold degeneracy. Splitting occurs when these seats become different and the symmetry changes to a lower one. With one seat increasing or decreasing, the other seats are influenced due to interlocking. Dependence of these seats on each other could be derived based on the sphere triangle functions. Degenerated seat levels

TABLE I. Seat Analysis for the Most Common Structural Patterns (compare with Fig. 2)[a]

Seat description		Structure pattern					
		Td	Oh	C	S.A.	T.B.[b]	P.B.[b]
S_1	n	4	6	8	8	3	2
	FA (°)	54.7	45	35.3	37.43	60	54
	Bond angle (°)	109.5	90	70.6	74.86	120	180
	SAS_{S_1}	0.8453	0.8787	0.7340	0.8236	0.7500	0.4122
S_2	n	4	8	6	2	2	5
	FA (°)	15.5	9.7	19.5	21.83	30	36
	Bond angle (°)	109.5	–	90	180	180	72
	SAS_{S_2}	0.073	0.057	0.1720	0.0717	0.1340	0.4775
Bond angle between S_1 and S_2		70.2	54.7	54.7	59.26	90	90
$SAS_{S_1+S_2}$		0.9183	0.9357	0.9096	0.8953	0.8840	0.8897
In all cases $\sum_{i=1}^{n} (SAF_{ir_i} = 0$							

[a]Abbreviations: SAS, the sum of the solid angle factors; FA, fan angle of the seats; n, number of the seats; $SAF_i r_i$, vector sum of the solid angle factors of the seats; Td, tetrahedron; Oh, octahedron; C, cubic; S.A., square antiprism; T.B., trigonal bipyramid; P.B., pentagonal bipyramid. [b]Fully interlocking.

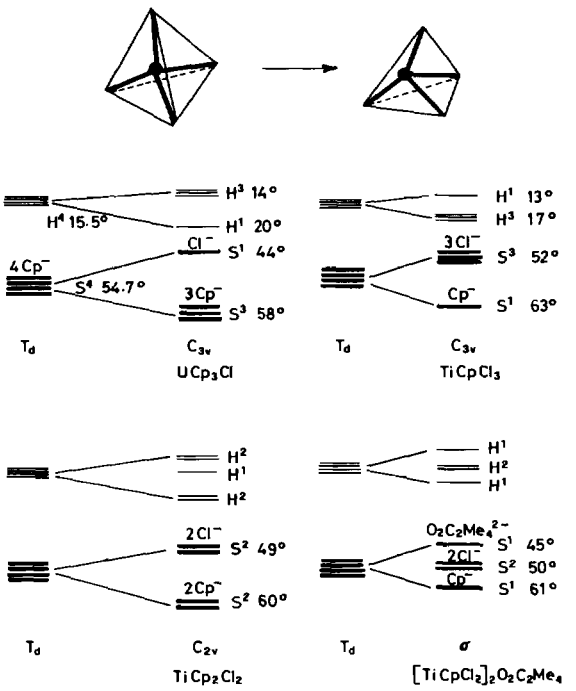

Fig. 3. Selected structural examples of distorted tetrahedra described with seat level diagrams.

are indicated by the closely arranged lines and the symbol S^n for a seat of n degeneracy.

Deformation of coordination polyhedra can be described with the seat level diagrams. Distortion from the regular polyhedra is always accompanied by the splitting of seat levels. The splitting of tetrahedral seats is taken as an example. While two of the four seats are increasing the other two seats must decrease. The previously four-fold degenerate seat levels split into two groups of seats, each of which possesses two-fold degeneracy. The splitting of the seat levels of distorted tetrahedral geometry is shown in Fig. 3. The dependence of seat A and seat B (at C_{2v} symmetry) in the A_2B_2 group of cones is shown in Fig. 4.

3. The Transformation of Symmetries on Variation of the Seats – Numerical Analysis of the Symmetry of Cones

The seats are not of constant value for they could be produced and expanded or contract and vanish. The first order seat could gradually decrease and become a second order and even a higher order seat. Meanwhile the second or the third order seat could increase and become the first order seat. Such processes are accompanied by the crossing of the seat levels and the transformation of the symmetries.

In fact, this is a problem of the numerical analysis of the symmetry of cones which are interlocked into each other in the 4π bonding space. The symmetry

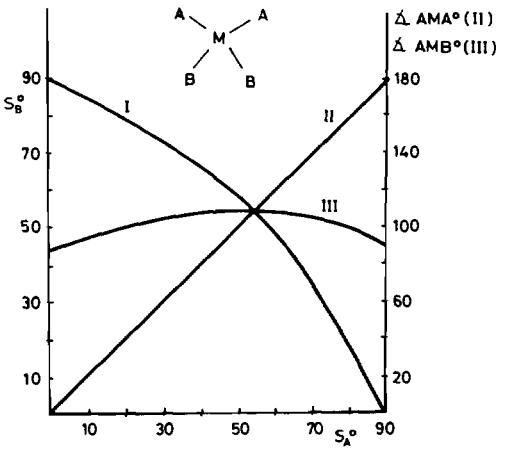

Fig. 4. Seats and geometrical frame of molecules MA_2B_2. Abscissa, seat A; ordinate on the left, seat B; ordinate on the right, bond angle; curve I, dependence of seat B on seat A; curve II, dependence of bond angle AMA on seat A; curve III, dependence of bond angle AMB on seat A.

of cones differs from the symmetry of points in that there are interrelations between the symmetry and the size of the cones. The relationship is illustrated using a group of four cones composed of three A cones and one B cone (Fig. 5 and Table II). When

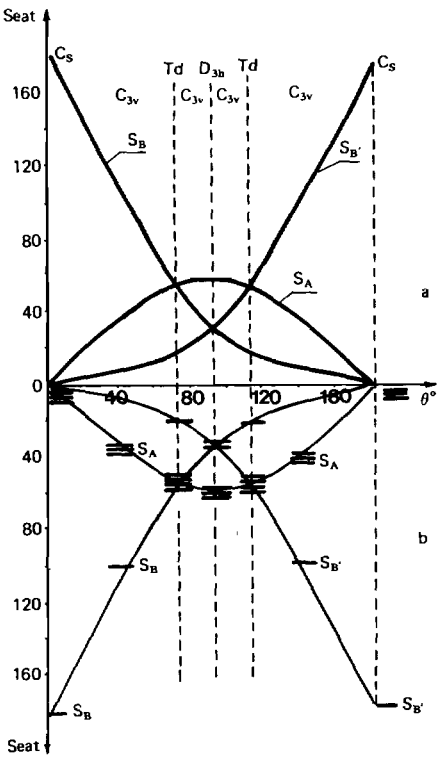

Fig. 5. Seat level diagram for MA_3B packing. (a) Changes of seats in correlation with the geometrical frame and the symmetries. (b) Changes of the seat level diagram corresponding to (a). Abscissa, angle θ = angle between axis and seat A.

TABLE II. Seats and the Correlated Geometrical Frame of MA_3B[a]

θ (°)	0	30	50	60	65	70	70.35	75	80	85	90	100	150	170
Angle AOB(180–θ) (°)	180	150	130	120	115	110	109.47	105	100	95	90	80	30	10
Angle AOA (°)	0	51.31	83.12	97.18	103.42	108.93	109.47	113.55	117.05	119.25	120	117.05	51.31	17.29
S_A (°)	0	25.66	41.56	48.59	51.71	54.46	54.74	56.77	58.53	59.62	60	58.52	25.66	8.65
S_B (°)	180	124.34	88.44	71.41	63.29	55.54	54.74	48.23	41.47	35.37	30	21.48	4.34	1.35
$S_{B'}$ (°)	0	4.34	8.43	11.41	13.2	15.53	15.79	18.22	21.47	25.38	30	41.48	124.4	161.35
SAS_{A+B}	1	0.9314	0.8692	0.8583	0.8590	0.8634	0.8443	0.8700	0.8769	0.8819	0.8840	0.8767	0.9314	0.9909

[a]For abbreviations see Table I.

seat A is zero, the whole space is occupied by seat B ($S_B = 180°$). All the other seats are zero. When the seats A increase gradually, seat B decreases synchronically. At the first stage, seat B is the largest seat and seat A the next largest. The cone seats which are interlocked in the holes among the two seats A and one seat B are in the third level and those among the three seats A are in the fourth level. When the three A seats have expanded to equal seat B, the geometrical frame achieves T_d symmetry. The seat levels for A and B are equivalent and they are in a four-fold degenerate state. Meanwhile seat B′ and the other three seats among AAB become identical. Subsequently the seats A continue to expand, becoming the largest ones and seat B contracts becoming the second largest seat while seat B′ rises to the third largest seat. At the point when the seats A increase to 60°, the seat B′ rises to become the same as the seat B. Both of them are 30°. The symmetry of the geometrical frame then becomes D_{3h}. The seats A are at their maximum at D_{3h} symmetry and decrease afterwards. The geometrical frame turns over in the direction of MB (see Fig. 5). The seat B becomes smaller than seat B′, which gradually increases to become equal to seat A. The symmetry then reverts to T_d. The process continues until seat B′ becomes the largest one and then finally occupies the whole space and the other seats vanish. During the whole process the symmetry changes in the following sequence:

$$C_s \longrightarrow C_{3v} \longrightarrow T_d \longrightarrow C_{3v} \longrightarrow D_{3h} \longrightarrow C_{3v} \longrightarrow T_d \longrightarrow C_{3v} \longrightarrow C_s$$

Crossing of the seat levels occurs many times, each time accompanied by the change of symmetries and inversion of seat orders. The functional dependence of the main seats is as follows:

$$\begin{aligned} &2\cos(2S_A) = 3\cos^2(S_A + S_B) - 1 \\ &\text{angle AOB} = S_A + S_B \\ &\text{angle AOA} = 2S_A \\ &\text{angle AOB}' = S_A + S_B' \end{aligned} \tag{2}$$

4. Occupied Seats and Unoccupied Seats

Due to non-bonding repulsions, in weak CFSE ligands tend to occupy as much coordination space as possible. The space occupancy indicated by the Solid Angle Factor Sum (*SAS*) of the ligand-occupied seat could be used for estimation of the relative stability of different isomers.

For example, there is another pattern of four cone packing in D_{4h} symmetry. We can describe the

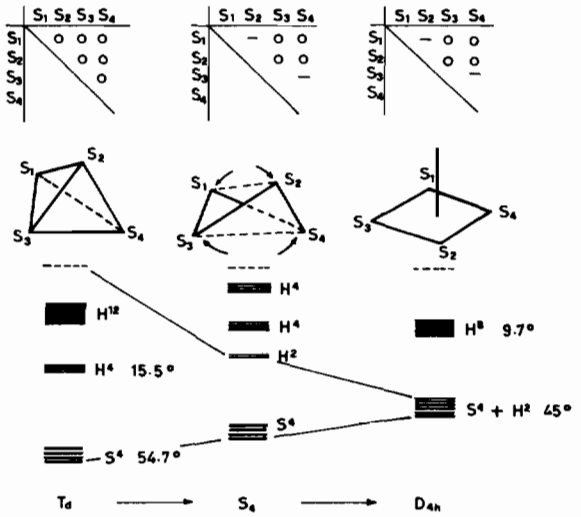

Fig. 6. Isomerism in four ligand packing: from tetrahedron to tetragon.

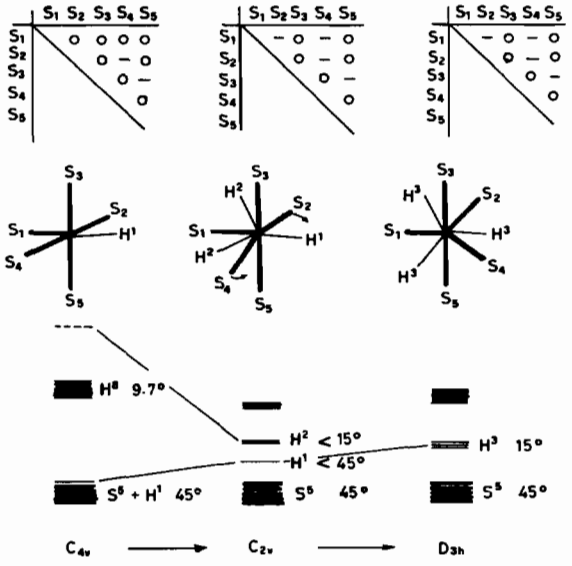

Fig. 7. Isomerism in five ligand packing (MA_5 type): from square pyramid to trigonal bipyramid.

seat interlocking by the matrices shown in Fig. 6. In the matrices the symbol O indicates the two seats are in contact with each other whereas the short line indicates that the seats are separated. The four identical seats are in T_d symmetry when they interlock completely. They become smaller in a squeezed tetrahedron when the interlockings between S_1 and S_2, and between S_3 and S_4 are broken down. When the tetrahedron was squeezed to become a tetragon, each seat possesses a fan angle of only 45°. The *SAS* value for the occupied seats had decreased from 0.845 to 0.586. Meanwhile one can see from Fig. 6 that the difference between the largest unoccupied seat and the occupied seat decreases gradually during the process of squeezing. In a tetrahedron the difference is 29.2° whereas in a tetragon the difference is zero. Normally, the larger the vacant seat and the smaller the occupied seat, the easier the ligand migrates from the latter to the former. When a vacant seat is equal to the occupied seats the ligand should move freely and the structure should be completely fluxional provided that there is no restriction of electronic effect. The square planar structure is stable only for central ions with d^n and p^n electron configuration. When the central ions have lost all their valence shell electrons, the steric factor becomes dominant and tetrahedral structures become more stable.

In this case the packing of three ligands should adopt D_{3h} symmetry rather than C_{3v} symmetry because the largest vacant seats reach a minimum of 30° at D_{3h} symmetry and become larger in C_{3v} symmetry. The occupied seats become smaller than 60°, so that the difference decreases on changing from D_{3h} to C_{3v}.

The seat analysis shows that it is impossible to produce five identical seats interlocking each other without producing large vacant seats. In a square pyramid both the five occupied seats and the remaining vacant seat are 45° so that the frame is fluxional. For the trigonal bipyramid if the equatorial seats are the same size as the axial seats, they will reach at maximum 45°. These equatorial seats cannot be fixed completely by interlocking with each other because the sum of the fan angles of the three seats is 135° only (Fig. 7).

It is therefore expected that neither in ionic lattice nor in coordination compounds of the first class of metal ions, which had lost all its valence electrons, will a molecular structure composed of five identical metal–ligand bonds be stable. In packing of five ligands made up by four ligands A and one ligand B, two sets of seats will generate according to whether the ligand A is larger or smaller than the ligand B. If $A < B$ the seat level diagram (Fig. 8) shows that the largest seat is S_B, with the four-fold degenerated S_A next to it. The largest vacant seat H nevertheless competes with the occupied A seats. This vacant seat has a strong tendency to accommodate ligands to reach a pseudo-O_h coordination pattern. If ligand A is larger than ligand B, an inverted square pyramid will result (Fig. 8) with the metal atom lying outside. Such a structure is not favoured because the vacant seat is even larger than the occupied ones. Interestingly, in actual molecular structures for the first class of metal ions, such a structure pattern has not been found so far. In packing of the five ligands made up by three A and two B when the fan angle of the ligand A is greater than that of the ligand B,

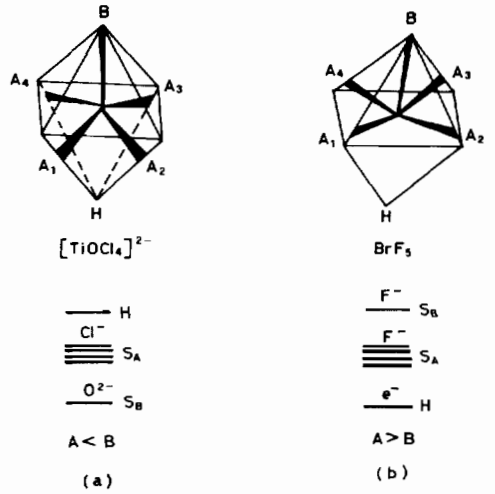

Fig. 8. Square pyramid of five ligand packing (MA_4B).

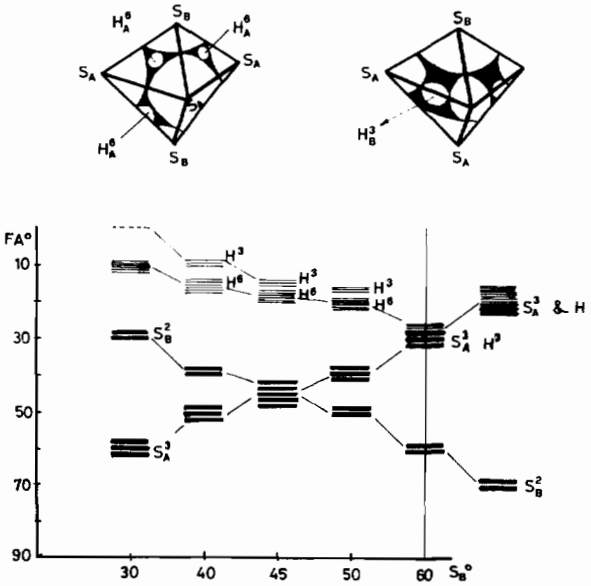

Fig. 9. Seat level diagram for three A seats and two B seats arranged in D_{3h} symmetry. Note: 1. The horizontal for showing the change of seat levels in accordance with S_B. 2. H_A and H_B are not independent empty seats, the angle between them is less than $H_A + H_B$. 3. When $S_B \geqslant 60°$, then S_A = H.

the frame symmetry would be D_{3h} (Fig. 9), of which the largest vacant seat is very small (10.9°) so that such a pattern is very stable. Experimental observation has confirmed this inference with several structures of MCp_3X_2 (M = U, La, Ce, Pr; X = MeCN, NCS). It is argued that the apical seats, S_B, are restricted to be small when seats S_A are large so that only small ligands could be accommodated in them. It should be noted that D_{3h} symmetry is not always the favoured one. When ligands B are larger than ligands A, the symmetry of C_{2v} is preferred rather than D_{3h} for ligand arrangement, such as in the structures of MCp_2H_3 (M = V, Ta). These could be explained in that a set of three A seats and two B seats has a higher space occupancy arranged in D_{3h} symmetry than in C_{2v} symmetry when $S_A > S_B$ (Fig. 10), whereas it has a higher space occupancy in C_{2v} symmetry when $S_B > S_A$. Dependences of S_B, and major vacant seats on S_A, in both symmetries, are shown in Fig. 10a. Space occupancies and the seat level diagrams are shown in Fig. 10b and c. An example is thus given to show the role of steric factors in ligand arrangement. It is also interesting to note that in packing of three big A cones and two small B cones, the 'side on' isomer has so far not been found. This isomer is unstable because a big vacant seat always accompanies the two seats of the B cones. Thus in C_{3v} symmetry when the two B cones are at the two cross sites with one relative to the three A seats, the

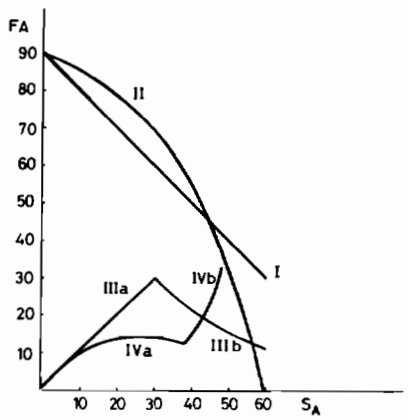

Fig. 10(a). Comparison of D_{3h} and C_{2v} arrangements of three A seats and two B seats. I, S_B in D_{3h} arrangement; II, S_B in C_{2v} arrangement; III, the largest vacant seat in D_{3h} arrangement; IIIa, the largest seat in the equatorial position; IIIb, the largest seat in the face centre of the triangle bipyramid; IV, the largest vacant seat in C_{2v} arrangement; IVa, the vacant seat among triangle A_2BB; IVb, the vacant seat among triangle A_1BB.

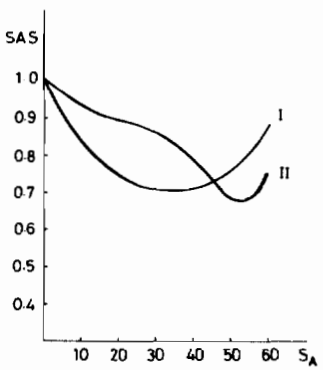

Fig. 10(b). Comparisons of D_{3h} (I) and C_{2v} (II) symmetry in space occupancy.

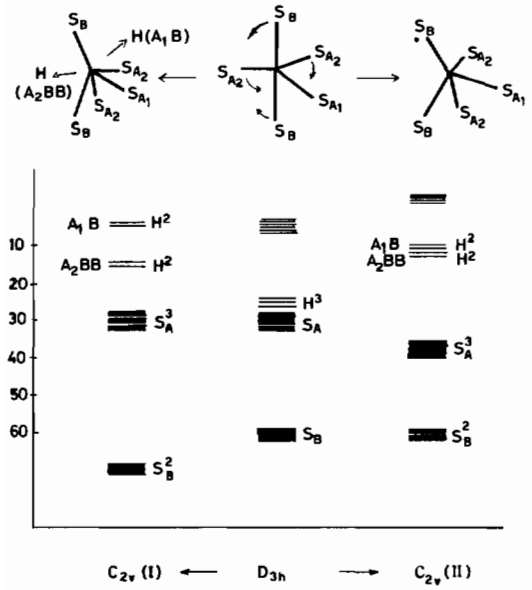

Fig. 10(c). Degradation of D_{3h} to C_{2v} in ligand packing. C_{2v}(I), $S_A{}^3$ (in D_{3h}) = $S_A{}^3$ (in C_{2v}); $S_B{}^2$ (in D_{3h}) < $S_B{}^2$ (in C_{2v}); C_{2v}(II), $S_B{}^2$ (in D_{3h}) = $S_B{}^2$ (in C_{2v}); $S_A{}^3$ (in D_{3h}) < $S_A{}^3$ (in C_{2v}).

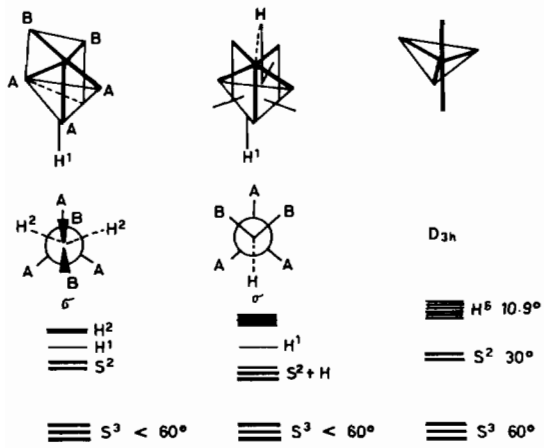

Fig. 11. Isomerism in correlation with the difference between the smallest occupied seat and the largest vacant seat: MA_3B_2 (A > B) packing.

third cross site will be left empty; in σ symmetry one of the B cones is at the cross site while another is at the *syn* site (Fig. 11); the two partially occupied empty sites still have larger holes than those holes in the D_{3h} arrangement.

Another example is illustrated in the six-cone packing. When the seats are arranged in octahedral symmetry, the fan angles of the occupied seats will be 45° and the empty seat will be 9.6°. However when the six cones are arranged in a trigonal prism the occupied seats will decrease to 41° while the vacant seats at the center of the three tetragons will increase to 26.8°. The fact simply means that the spaces distributed to the cones are less and the waste space left for the holes has increased in the trigonal prism. It is thus concluded that in the ideal steric packing, the octahedral arrangement is more favourable than the trigonal prism. This conclusion is supported by the fact that unless the ligands are bidentate the trigonal prism is very unusual.

In packing of eight ligands (MA_8), *SAS* values are 0.734 and 0.824 for cubic and square antiprism. The difference between the occupied seat and the largest vacant seat is 15.8° and 15.6° respectively. Whereas there are six large empty seats in a cubic structure, there are only two large vacant seats in square antiprismatic structure. The square antiprism, therefore, is more favourable than the cubic.

Acknowledgements

This work was supported both by the Natural Science Foundation of the Chinese Government and by the Open Laboratory Research Fund of the University of Science and Technology of China.

We thank Professor M. F. Richardson and Professor J. Müller for helpful discussion and for English revision.

We are extremely grateful to Professor K. W. Bagnall of Manchester University, for his tremendous help in careful reading and revision of our original manuscripts.

References

1 C. A. Tolman, *J. Am. Chem. Soc., 92,* 2956 (1970).
2 C. A. Tolman, *Chem. Rev., 77,* 313 (1977).
3 S. N. Titova, V. T. Bychkov, G. A. Domrachev and Y. T. Struckov, *Inorg. Chim. Acta, 50,* 71 (1981).
4 A. J. Smith, G. Bombieri, G. de Paoli and P. Zanella (eds.), 'Proc. 11èmes Journées des Actinides, Lido de Jesolo, Italy, May 25–27, 1981', C.N.R. Padua, Italy, 1982, p. 64.
5 (a) Li Xing-fu, *Ph.D. Qualification Research Report,* University of Manchester, 1980; (b) Li Xing-fu, *Ph.D. Thesis,* University of Manchester, 1982; (c) K. W. Bagnall and Li Xing-fu, *J. Chem. Soc., Dalton Trans.,* 1365 (1982).
6 E. B. Lobkovskii, *Zh. Khim., 24,* 66 (1983).
7 Li Xing-fu and R. D. Fischer, *Inorg. Chim. Acta, 94,* 50 (1983).
8 R. D. Fischer and Li Xing-fu, *J. Less-Common Met., 112,* 303 (1985).
9 (a) Li Xing-fu, Feng Xi-zhang, Xu Ying-ting, Sun Peng-nian and Shi Jie, *Acta Chim. Sin., 43,* 502 (1985) (in Chinese); (b) Feng Xi-zhang, Guo Ao-ling, Xu Ying-ting, Wang Hi-ding, Liu Li, Shi Jie, Li Xing-fu and Sun Peng-nian, *Polyhedron,* 1987, in press.
10 Li Xing-fu, Feng Xi-zheng, Xu Ying-ting, Wang Hai-dung, Shi Hie, Liu Li and Sun Peng-nian, *Inorg. Chim. Acta, 117,* 85 (1986).
11 Wang Ling-jin, Xu Ying-ting, Shen Tian-ji, Guo Ao-ling and Li Xing-fu, *Polyhedron,* 1987, in press.
12 Li Xing-fu, Xu Ying-ting, Feng Xi-zhang, Guo Ao-ling and Sun Peng-nian, *J. Mol. Sci., 5,* 159 (1987).
13 Li Xing-fu, Xu Ying-ting, Feng Xi-zhang and Sun Peng-nian, *Inorg. Chim. Acta, 116,* 75 (1986).